CHAPTER 4

Effects of global change on inflorescence production: a Bayesian hierarchical analysis

Janneke Hille Ris Lambers, Brian Aukema, Jeff Diez, Margaret Evans, and Andrew Latimer

The effects of global change on seed production may dramatically impact plant community composition, because species-specific recruitment rates influence species diversity, successional trajectories and invasion rates. We developed a Bayesian hierarchical model to quantify the effects of three global change factors (elevated CO_2, nitrogen deposition, and declining diversity) on allocation to inflorescence production of 12 grassland species. We used the results from these analyses to consider (1) how seed production might be affected by global change and (2) whether species within functional groups respond similarly to global change. We found that all three global change factors affected allocation to inflorescence production in different ways. Elevated CO_2 decreased the number of inflorescences per unit biomass for all species, although 95% credible intervals overlapped zero for seven of twelve species. Increased nitrogen had both positive (five species) and negative effects (two species) on the number of inflorescences per unit biomass. There were also positive (two species) and negative (three species) effects of declining diversity on allocation to inflorescence production. Only the effects of nitrogen on inflorescence allocation could be generalized to functional groups: C3 grasses generally decreased allocation to inflorescence production with increased nitrogen, while C4 grasses increased allocation to inflorescence production under elevated nitrogen. The cause of this response is unclear, as other traits besides photosynthetic pathway differentiate C3 grasses from C4 grasses in this system (e.g. clonality, seasonality). Overall, our results suggest that global change will strongly affect seed production of grassland species, and that categorizing those responses by ecophysiological traits is probably not desirable. We also discuss the advantages a Bayesian hierarchical framework has over classical statistical models in analyzing these data.

4.1 Introduction

The effects of global change on plant community dynamics will depend on how factors such as elevated CO_2, nitrogen deposition, and the loss of diversity differentially affect plant species within those communities. Understanding the effects of these global change factors on seed production may be particularly important, because differences among plant species at early life history stages are thought to play an important role in maintaining species diversity (Shmida and Ellner 1984; Tilman 1994; Hurtt and Pacala 1995; Turnbull et al. 2000), determining successional trajectories (Gleeson and Tilman 1990; Fastie 1995; Fuller and del Moral 2003), and driving the rate of spread of invasive species (Smith et al. 2000, Richardson and Rejmanek 2004). If global change factors such as elevated CO_2, nitrogen deposition, and species loss affect seed production in a species-specific manner, plant community characteristics may be dramatically affected. Unfortunately, we know little about the implications of global change for seed production, because the species-specific effects of global

GELFAND: "CHAP04" — 2006/3/20 — 16:57 — PAGE 59 — #1

change factors such as CO_2, nitrogen, and diversity are usually estimated only for aboveground vegetative characteristics, such as relative growth and productivity (DeLucia et al. 1999; Isebrands et al. 2001; Reich et al. 2001; Tilman et al. 2001; Norby et al. 2002; Reich et al. 2004; but see Smith et al. 2000; LaDeau and Clark 2001; Thurig et al. 2003).

In this chapter, we ask whether reproduction of Midwestern grassland species is affected by elevated CO_2, nitrogen deposition, and species diversity. Specifically, we examine the relationship between aboveground biomass and number of inflorescences (i.e. reproductive allocation, one measure of seed production) in an experiment that manipulates CO_2, nitrogen, and diversity in a fully factorial design. We expected that plants would allocate more biomass to reproduction (inflorescence production) than growth and survival as the supply of limiting resources, such as CO_2 and nitrogen, increase (Navas et al. 1997; Gardner and Mangel 1999; Hautekeete et al. 2001). We further expected that the magnitude of these shifts would depend on ecophysiology, summarized here in terms of functional groups. We predicted that allocation to inflorescence production of nitrogen-fixing legumes would respond most strongly to elevated CO_2, followed by C3 forbs and grasses, while C4 grasses would be relatively insensitive to elevated CO_2 (Wand et al. 1999; Poorter and Navas 2003). We also hypothesized that allocation to inflorescence production of C3 grasses and forbs, generally the plants most limited by nitrogen in these grasslands, would increase most strongly with the addition of nitrogen, while reproductive allocation of C4 grasses (strong soil N-competitors) and legumes would not be affected by the addition of this limiting resource. We did not have strong expectations for how inflorescence production might be affected by declining diversity, because plot diversity correlates with numerous abiotic (light, water, nutrient) as well as biotic factors (competition, the prevalence of mutualists and natural enemies) that might influence allocation to reproduction.

We developed our statistical model using a Bayesian hierarchical approach. Although our data were collected from a large-scale manipulative experiment designed to meet the requirements of frequentist statistics, there were several reasons we chose to implement a hierarchical Bayesian approach instead. First, we wished to estimate species-specific and overall effects of global change on inflorescence production while accommodating plot-level, ring-level, and species-level variability as random effects. Second, we wanted percent cover data, another measure of species abundance, to inform estimates of aboveground biomass in our statistical model. Finally, we wished to include sampling error in the modeling of our covariates: biomass and percent cover (assumed to be measured without error in classical analysis). Accomplishing these goals using traditional statistical analyses (e.g. multiple regression and analysis of variance), used in many studies of these global change factors (e.g. DeLucia et al. 1999; Isebrands et al. 2001; Reich et al. 2001; Tilman et al. 2001; but see LaDeau and Clark 2001), was not possible.

4.2 Methods

4.2.1 Experimental design and data

The BioCON experiment (Biodiversity, CO_2 and Nitrogen—http://www.lter.umn.edu/biocon/) was established in 1997 on a former agricultural field in central Minnesota that had been abandoned in the 1970s. Figure 4.1 illustrates the experimental design. Before plots were established, the existing vegetation was removed, and soils were treated with methyl bromide to kill seeds in the soil seed bank. Each 2 m $\times$ 2 m plot was seeded with 48 g of seed (equally divided among component species) in 1997, and diversity levels were maintained by annual weeding. CO_2 and nitrogen treatments were initiated in 1998.

The experiment consists of a fully factorial combination of CO_2 treatments (ambient at 367 ppm, and elevated at 550 ppm), nitrogen treatments (ambient versus 4 g nitrogen per m^2 per year), and species richness treatments (1, 4, 9, and 16 species). CO_2 treatments were applied to six rings (three ambient, three elevated) using the FACE (Free Air Carbon dioxide Enrichment) technology (Figure 4.1). CO_2 was added during daylight hours over the entire growing season, approximately mid-April to mid-October. Nitrogen and species richness treatments were replicated in the 61 4 m^2 plots within each ring (Figure 4.1). Nitrogen was added at three dates annually in the form of NH_4NO_3. For

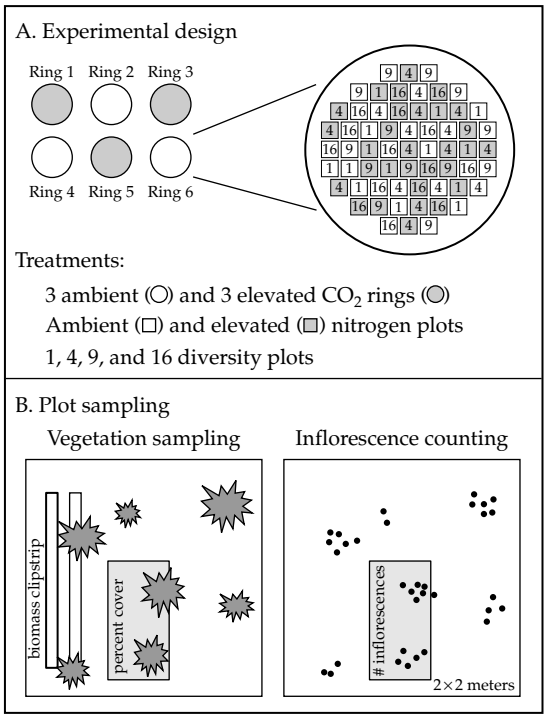

Figure 4.1. Experimental design of the BioCON experiment (a), and sampling of one hypothetical species within one plot (b). Large circles represent rings in (a), which are replicated six times on an abandoned agricultural field. Two-meter high pipes surrounding rings continuously emit air at ambient levels in three rings (367 ppm; open circles), and at elevated CO_2 levels in the other three rings (550 ppm; hatched circles). Each ring contains 61 4-m^2 plots (small squares in (a)). Half of the plots within each ring receive additional nitrogen annually (gray shaded squares in (a)) to mimic nitrogen deposition. Plots were planted with 16, 9, 4, or 1 of the total pool of 16 species. Within each plot (b), aboveground biomass of all species was harvested from two different 0.1×1.5 meter clipstrips in June and August of 2002, and percent cover was assessed at the same time in an adjacent 0.5×1 meter quadrat (grey rectangle). Inflorescences were counted for all species in percent cover quadrats at the time of reporductive maturity. Irregular stars and black dots represent vegetative biomass and inflorescences of a hypothetical species (b).

each CO_2 and nitrogen treatment combination, there were 32 monoculture plots, 15 four-species plots, 15 nine-species plots, and 12 sixteen-species plots. All of the 16-species plots in this experiment were composed of the same late-successional perennial herbaceous species. Each species occurred in two monoculture plots per nitrogen and CO_2 treatment, while species composition of four- and nine-species plots was determined by a separate random draw from the pool of species.

The 16 species in the experiment were all late-successional, herbaceous, perennial species representing four functional groups. We restricted our analyses to the twelve most abundant species in the experiment (the other four species were rarely found outside of monoculture plots). These species included C3 grasses (*Agropyron repens, Bromus inermis, Koeleria cristata, Poa pratensis*), C4 bunchgrasses (*Andropogon gerardii, Bouteloua gracilis, Schizachyrium scoparium, Sorghastrum nutans*), forbs (*Achillea millefolium, Solidago rigida*), and nitrogen-fixing legumes (*Lespedeza capitata, Lupinus perennis*). We counted the number of inflorescences of each species (at the time of seed dispersal) within a $0.5\ m \times 1.0\ m$ quadrat within each plot (Figure 4.1). Two measures of the abundance of each species within each plot were also collected: percent cover in a $0.5\ m \times 1.0\ m$ quadrat (the same quadrat where reproductive inflorescences were counted) and grams of aboveground biomass per m^2 from a $1.5\ m \times 0.1\ m$ clip strip adjacent to permanent quadrats (Figure 4.1). Biomass and percent cover data were collected in June and August of 2002. In all, our data consist of 1446 species- and plot-specfic counts of inflorescences per m^2 and 2892 observations of species- and plot-specific percent cover and aboveground biomass per m^2. Each species was found in 116–126 of the 366 4 m^2 plots.

4.2.2 Hierarchical Bayesian model structure

We developed a hierarchical Bayes model to estimate how allocation to inflorescence production responds to elevated CO_2, nitrogen deposition, and declining diversity (Figure 4.2). Because we were interested in the effects of global change on allocation to reproduction, rather than its effects on the productivity of individual species, we estimated the effects of these three global change factors on the relationship between biomass and inflorescences (rather than on the number of inflorescences per m^2 or on biomass produced per m^2). We used three types of data collected at the plot level (Figure 4.1): counts of inflorescences per species per unit area, the amount of vegetative biomass produced per species per unit area (two observations per plot), and visual estimates of the percent cover of each species in each plot (two observations per plot). Although we wished to

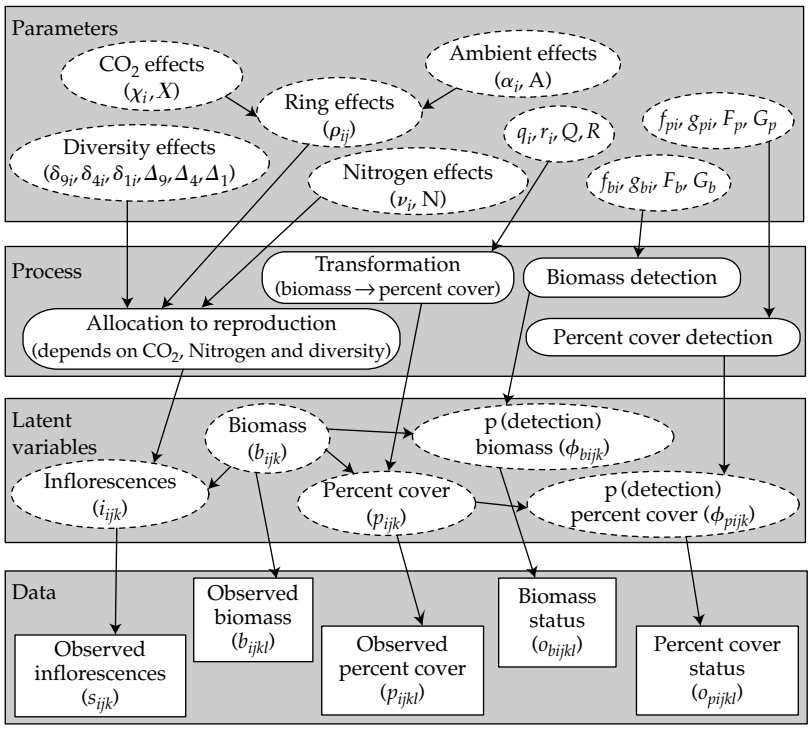

Figure 4.2. Hierarchical Bayes model structure for the analysis of per unit biomass inflorescence production, as affected by elevated CO_2, nitrogen deposition, and declining diversity. Gray boxes indicate different hierarchical levels of the model, white squares indicate observed data, and white circles bordered with dashed lines indicate model elements estimated by Gibbs sampling. Oval white boxes represent the four process models in our analysis. Arrows indicate how parameters, process, and data are related.

model the relationship between biomass (a function of the total number and size of individual plants within plots) and inflorescences, biomass is measured over a smaller area than percent cover, and, contrary to percent cover, measured in a different area than inflorescences are counted (Figure 4.1). Thus, we used percent cover data to provide additional information on the abundance of each species in each plot (Figure 4.3(b,e,h,k)).

Our hierarchical Bayes model consists of (1) data models (describing sampling distributions of observed inflorescences, biomass and percent cover), (2) process models (describing how inflorescence production is related to biomass and global change factors; and how biomass and percent cover data are related to the unobserved biomass of each species in each plot) and (3) parameter models (describing how species-specific parameters relate to population-level parameters and how population-level parameters relate to priors). In its simplest form, our model can be represented as follows:

$$\begin{aligned} &p(\text{parameters}|\text{data, priors}) \\ &\quad \propto p(\text{data}|\text{process, data parameters}) && \text{(4.1a)} \\ &\qquad \times p(\text{process}|\text{process parameters}) && \text{(4.1b)} \\ &\qquad \times p(\text{parameters}|\text{overall effects, priors}). && \text{(4.1c)} \end{aligned}$$

Our first data model relates the observed number of inflorescences of species i in ring j and plot k (s_{ijk}) to the expected (unobserved) number of inflorescences in that same plot (ι_{ijk}). We used a Poisson model because inflorescences are count data:

$$s_{ijk} \sim \text{Pois}(\iota_{ijk}). \tag{4.2}$$

Our inflorescence production process model, in turn, relates the expected number of inflorescences per m^2 of species i in ring j and plot k (ι_{ijk}) to the biomass produced by that species in that plot as

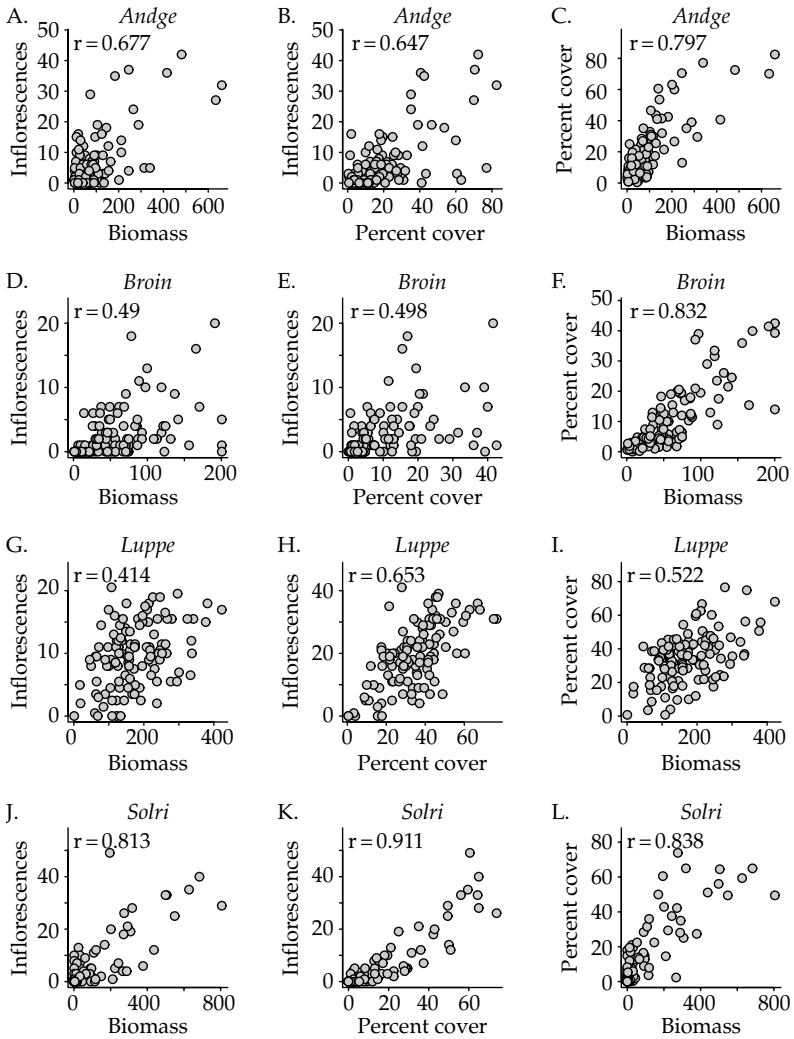

Figure 4.3. Scatterplots of raw data for four species: *A. gerardii* (a,b,c), *B. inermis* (d,e,f), *L. perennis* (g,h,i), and *S. rigida* (j,k,l). Figure 4.3(a,d,g,j) Shows the relationship between vegetative biomass ($\bar{b}_{ijk}$; the average of two measures) and inflorescences per m^2 (s_{ijk}), Figure 4.3(b,e,h,k) shows the relationship between percent cover ($\bar{p}_{ijk}$; also the average of two measures) and inflorescences per m^2 (s_{ijk}), and Figure 4.3(c,f,i,l) shows the relationship between vegetative biomass per m^2 ($\bar{b}_{ijk}$) and percent cover ($\bar{p}_{ijk}$).

well as parameters that describe how the relationship between biomass and inflorescences varies per ring and is affected by nitrogen and diversity:

$$\iota_{ijk} = \beta_{ijk} \exp(\rho_{ij} + \nu_i n_{jk} + \delta_{9i} d_{9jk} + \delta_{4i} d_{4jk} + \delta_{1i} d_{1jk}). \quad (4.3)$$

The parameter ρ_{ij} is the inflorescence production per unit biomass of species i in ring j under ambient nitrogen conditions in 16 species plots. The parameter ν_i describes how elevated nitrogen affects per unit biomass inflorescence production, and is multiplied by the dummy vector n_{jk}, a series of 1s and 0s identifying plots within rings as having nitrogen added (1) or not (0). The parameters δ_{9i}, δ_{4i}, and δ_{1i} describe how the different diversity treatments (relative to 16 species plots) affects per unit inflorescence production, and are multiplied by the

dummy vectors d_{9jk}, d_{4jk}, and d_{1jk} (respectively), a series of 1s and 0s identifying those plots at 9, 4, and 1 levels of diversity. Note that we chose to model biomass as being proportional to inflorescences, because the relationship between biomass and inflorescence data was not obviously nonlinear for the twelve species we analyze (e.g. Figure 4.3(a,d,g,j)). A saturating function probably better describes the relationship between individual plant size and fecundity (LaDeau and Clark 2001; detailed analysis available in Clark et al. 2004), but our data describe the relationship between biomass and fecundity (inflorescences) on an area, not individual basis.

Because elevated CO_2 was applied at the ring, not plot level (Figure 4.1), we estimated species-specific effects of elevated CO_2 on allocation to inflorescence production from ring-specific allocation parameters (i.e. the ρ_{ij}'s). Thus, our parameter model for ρ_{ij} in rings 2, 4, and 6 (rings exposed to ambient levels of CO_2; Figure 4.1) is a normal distribution with mean α_i and standard deviation σ_{ri}:

$$\rho_{ij} \sim \mathrm{N}(\alpha_i, \sigma_{ri}^2), \quad j = 2, 4, 6. \tag{4.4}$$

Similarly, our parameter model for ρ_{ij} in rings 1, 3, and 5 (rings exposed to elevated levels of CO_2; Figure 4.1) is a normal distribution with mean τ_i and standard deviation σ_{ri}:

$$\rho_{ij} \sim \mathrm{N}(\tau_i, \sigma_{ri}^2), \quad j = 1, 3, 5. \tag{4.5}$$

Inflorescence production per unit biomass in elevated rings (τ_i) is the sum of allocation in ambient rings (α_i) and the effect of elevated CO_2 on the production of inflorescences per unit biomass (χ_i):

$$\tau_i = \alpha_i + \chi_i. \tag{4.6}$$

The parameter σ_{ri} describes the ring-to-ring variation in per unit biomass inflorescence production of species i. We used the same variance parameter σ_{ri} for elevated and ambient rings, because we expected that ring-to-ring variation would not be affected by CO_2. Essentially, this model structure is a mixed effects model, with ring as a random effect.

Our second set of data and process models relate biomass observations b_{ijkl} of species i in ring j, plot k and sample l to expected (unobserved) biomass β_{ijk}. Observations of biomass (b_{ijkl}) that are greater than zero are drawn from a lognormal distribution with mean β_{ijk} and a species-specific standard deviation σ_{bi} (a species-specific parameter describing stochasticity when sampling biomass):

$$\log(b_{ijkl}) \sim N(\log(\beta_{ijk}), \sigma_{bi}^2), \quad b_{ijkl} > 0. \tag{4.7}$$

We assumed that species are present in all plots in which they were planted, and that observing no biomass in clipstrips results from a lack of detection rather than the extinction of the species from that plot. This is a reasonable assumption, because only four of the twelve species are absent as biomass, percent cover, and inflorescences in any plot (less than 3% of the total 1446 plots surveyed). We therefore modeled the status of biomass observations (o_{bijkl}, a vector of ones and zeros describing whether or not biomass was detected, that is, greater than zero, in clipstrips) as a Bernoulli sample from a parameter (ϕ_{bijk}), which describes the unobserved probability of detecting biomass greater than zero in that plot:

$$o_{bijkl} \sim \mathrm{Bern}(\phi_{bijk}). \tag{4.8}$$

Our process model for biomass detection links the probability of observing nonzero biomass in clipstrips (ϕ_{bijk}) to the expected (unobserved) biomass (β_{ijk}) in that plot and two parameters (f_{bi}, g_{bi}):

$$\mathrm{logit}(\phi_{bijk}) = f_{bi} + g_{bi} \log(\beta_{ijk}). \tag{4.9}$$

We chose not to estimate the effects of elevated CO_2, elevated nitrogen, and declining diversity on unobserved biomass (β_{ijk}; Figure 4.2), and gave all values of β_{ijk} the same diffuse prior (equation (4.26)). We did this because although CO_2, nitrogen, and diversity also affect aboveground biomass (Korner 2000; Reich et al. 2001; Hille Ris Lambers et al. 2004), we were primarily interested in estimating the effects of global change factors on allocation to reproduction, that is the production of inflorescences per unit biomass (regardless of whether global change affects biomass). Preliminary analysis (not shown) indicates that this simplifying assumption does not qualitatively affect parameters of interest (i.e. α_i, χ_i, ν_i, δ_{9i}, δ_{4i}, δ_{1i}).

Our third set of data and process models relate percent cover observations p_{ijkl} of species i in ring j, plot k, and sample l to the expected (unobserved) percent cover in that plot (π_{ijk}). For observations of percent cover that are greater than zero, we assume

a lognormal distribution with mean π_{ijk} and a standard deviation σ_{pi} (representing stochasticity when sampling percent cover):

$$\log(p_{ijkl}) \sim \mathrm{N}(\log(\pi_{ijk}), \sigma_{pi}^2), \quad p_{ijkl} > 0. \tag{4.10}$$

As with biomass, we modeled the status of percent cover observations (o_{pijkl}, a vector of ones and zeros describing whether or not percent cover was detected, that is greater than zero, in quadrats) as a Bernoulli sample from a plot-specific probability of observing percent cover values greater than zero (ϕ_{pijk}):

$$o_{pijkl} \sim \mathrm{Bern}(\phi_{pijk}). \tag{4.11}$$

Our percent cover detection model links the probability of observing percent cover that is greater than zero (ϕ_{pijk}) to the expected (unobserved) percent cover in that plot and two parameters (f_{pi}, g_{pi}):

$$\mathrm{logit}(\phi_{pijk}) = f_{pi} + g_{pi} \log(\pi_{ijk}). \tag{4.12}$$

Finally, we link percent cover of species i in ring j and plot k (π_{ijk}) to the biomass of that same species in plot j and ring k and two parameters (q_i and r_i) in our percent cover process model:

$$\log(\pi_{ijk}) = q_i + r_i \log(\beta_{ijk}). \tag{4.13}$$

Note that this relationship does not constrain percent cover to be less than 100. However, since percent cover observations for all species were far less than 100 (less than 1% of all percent cover observations are greater than 90), this simplifying assumption is reasonable.

We were also interested in determining whether the effects of the three global change parameters could be generalized. In other words, we wished to estimate the average effects of elevated CO_2, nitrogen deposition, and declining diversity on inflorescence production per unit biomass across all species (essentially equivalent to estimating the effects of global change when designating species as a random effect in a mixed model). Thus, we modeled parameters describing the species-specific relationship between biomass and inflorescences and effects of global change on this relationship ($\alpha_i, \chi_i, \nu_i, \delta_{9i}, \delta_{4i}, \delta_{1i}$) as independent normal distributions with means ($\mathrm{A}, \mathrm{X}, \mathrm{N}, \Delta_9, \Delta_4, \Delta_1$) and standard deviations ($\sigma_a, \sigma_c, \sigma_n, \sigma_d, \sigma_d,$ and σ_d):

$$\alpha_i \sim \mathrm{N}(\mathrm{A}, \sigma_a^2) \tag{4.14}$$

$$\chi_i \sim \mathrm{N}(\mathrm{X}, \sigma_c^2) \tag{4.15}$$

$$\nu_i \sim \mathrm{N}(\mathrm{N}, \sigma_n^2) \tag{4.16}$$

$$\delta_{9i} \sim \mathrm{N}(\Delta_9, \sigma_d^2) \tag{4.17}$$

$$\delta_{4i} \sim \mathrm{N}(\Delta_4, \sigma_d^2) \tag{4.18}$$

$$\delta_{1i} \sim \mathrm{N}(\Delta_1, \sigma_d^2) \tag{4.19}$$

Species-specific diversity treatment effects ($\delta_{9i}, \delta_{4i}, \delta_{1i}$) share a common standard deviation (σ_d) because we felt data were not extensive enough to estimate separate standard deviations for each diversity treatment effect.

We also modeled parameters describing the relationship between biomass, percent cover, and the probabilities of sampling biomass and percent cover ($f_{bi}, f_{pi}, g_{bi}, g_{pi}, q_i, r_i$) as normal distributions with global means (F_b, F_p, G_b, G_p, Q, R) and independent standard deviations ($\sigma_{bf}, \sigma_{pf}, \sigma_{bg}, \sigma_{pg}, \sigma_q, \sigma_r$):

$$f_{bi} \sim \mathrm{N}(F_b, \sigma_{bf}^2) \tag{4.20}$$

$$f_{pi} \sim \mathrm{N}(F_p, \sigma_{pf}^2) \tag{4.21}$$

$$g_{bi} \sim \mathrm{N}(G_b, \sigma_{bg}^2) \tag{4.22}$$

$$g_{pi} \sim \mathrm{N}(G_p, \sigma_{pg}^2) \tag{4.23}$$

$$q_i \sim \mathrm{N}(Q, \sigma_q^2) \tag{4.24}$$

$$r_i \sim \mathrm{N}(R, \sigma_r^2) \tag{4.25}$$

We were primarily interested in borrowing strength across species in mean effects, particularly for global change parameters (equations (4.14)–(4.19)), thus, we did not model species-level variance parameters (e.g. $\sigma_{bi}, \sigma_{pi}, \sigma_{ri}$) with global means.

Combining our data, process, and parameter models leads to the following joint posterior (where

"…" represent parameter priors):

$$
\begin{aligned}
& p\left(\begin{array}{l}\beta_{ijk}, \rho_{ij}, \alpha_i, \chi_i, \delta_{9i}, \delta_{4i}, \delta_{1i}, \nu_i, f_{bi}, f_{pi}, g_{bi}, g_{pi}, q_i, r_i, \\ \mathrm{A}, \mathrm{X}, \Delta_9, \Delta_4, \Delta_1, \mathrm{N}, F_b, F_p, G_b, G_p, Q, R, \\ \sigma_{bi}, \sigma_{pi}, \sigma_{ri}, \sigma_\alpha, \sigma_c, \sigma_d, \sigma_n, \sigma_{bf}, \sigma_{pf}, \sigma_{bg}, \sigma_{pg}, \sigma_q, \sigma_r \end{array} \middle| \right. \\
& \quad \left. b_{ijkl}, p_{ijkl}, o_{bijkl}, o_{pijkl}, s_{ijk}, \ldots \right) \\
& \propto \prod_{i=1}^{12} \prod_{j=1}^{6} \prod_{k=1}^{m_{ij}} \mathrm{Pois}\left[s_{ijk} \middle| (\iota_{ijk} | \alpha_i, \chi_i, \delta_{9i}, \delta_{4i}, \delta_{1i}) \right] \\
& \times \prod_{i=1}^{12} \prod_{j=1}^{6} \prod_{k=1}^{m_{ij}} \prod_{l=1}^{2} \mathrm{N}\left[\log(b_{ijkl}) \middle| (\log(\beta_{ijk}), \sigma_{bi}); \right. \\
& \quad \left. b_{ijkl} > 0 \right] \\
& \times \prod_{i=1}^{12} \prod_{j=1}^{6} \prod_{k=1}^{m_{ij}} \prod_{l=1}^{2} \mathrm{N}\left[\log(p_{ijkl}) \middle| [(\log(\pi_{ijk}) | q_i, r_i), \sigma_{pi}]; \right. \\
& \quad \left. p_{ijkl} > 0 \right] \\
& \times \prod_{i=1}^{12} \prod_{j=1}^{6} \prod_{k=1}^{m_{ij}} \prod_{l=1}^{2} \mathrm{Bern}\left[o_{bijkl} \middle| (\phi_{bijk} | f_{bi}, g_{bi}) \right] \\
& \times \prod_{i=1}^{12} \prod_{j=1}^{6} \prod_{k=1}^{m_{ij}} \prod_{l=1}^{2} \mathrm{Bern}\left[o_{pijkl} \middle| (\phi_{pijk} \middle| f_{pi}, g_{pi}) \right] \\
& \times \prod_{i=1}^{12} \prod_{j=1}^{6} \prod_{k=1}^{m_{ij}} \mathrm{N}(\log(\beta_{ijk}) | 4, 10) \\
& \times \prod_{i=1}^{12} \prod_{j=1,3,5} \mathrm{N}(\rho_{ij} | \alpha_i, \sigma_{ri}) \\
& \times \prod_{i=1}^{12} \prod_{j=2,4,6} \mathrm{N}\left[\rho_{ij} | (\alpha_i + \chi_i), \sigma_{ri} \right] \\
& \times \prod_{i=1}^{12} \mathrm{N}(\alpha_i | \mathrm{A}, \sigma_a) \prod_{i=1}^{12} \mathrm{N}(\chi_i | \mathrm{X}, \sigma_c) \\
& \times \prod_{i=1}^{12} \mathrm{N}(\nu_i | \mathrm{N}, \sigma_n) \prod_{i=1}^{12} \mathrm{N}(\delta_{9i} \middle| \Delta_9, \sigma_d) \\
& \times \prod_{i=1}^{12} \mathrm{N}(\delta_{4i} \middle| \Delta_4, \sigma_d) \prod_{i=1}^{12} \mathrm{N}(\delta_{1i} \middle| \Delta_1, \sigma_d) \\
& \times \prod_{i=1}^{12} \mathrm{N}(f_{bi} | F_b, \sigma_{fb}) \prod_{i=1}^{12} \mathrm{N}(f_{pi} | F_p, \sigma_{fp}) \\
& \times \prod_{i=1}^{12} \mathrm{N}(g_{bi} | G_b, \sigma_{gb}) \prod_{i=1}^{12} \mathrm{N}(g_{pi} | G_p, \sigma_{fp}) \\
& \times \prod_{i=1}^{12} \mathrm{N}(q_i | Q, \sigma_q) \prod_{i=1}^{12} \mathrm{N}(r_i | R, \sigma_r) \\
& \times \prod_{i=1}^{12} \mathrm{IG}(\sigma_{bi}^2 | 1, 0.1) \prod_{i=1}^{12} \mathrm{IG}(\sigma_{pi}^2 | 1, 0.1) \\
& \times \prod_{i=1}^{12} \mathrm{IG}(\sigma_{ri}^2 | 1, 0.1) \\
& \times \mathrm{N}(\mathrm{A} | 0, 3) \mathrm{N}(\mathrm{X} | 0, 3) \mathrm{N}(\mathrm{N} | 0, 3) \mathrm{N}(\Delta_9 | 0, 3) \\
& \times \mathrm{N}(\Delta_4 | 0, 3) \mathrm{N}(\Delta_1 | 0, 3) \mathrm{N}(F_b | 0, 3) \mathrm{N}(F_p | 0, 3) \\
& \times \mathrm{N}(G_b | 0.1, 3) \mathrm{N}(G_p | 0.1, 3) \mathrm{N}(Q | 0, 3) \\
& \times \mathrm{N}(R | 0.1, 3) \mathrm{IG}(\sigma_a^2 | 1, 0.1) \mathrm{IG}(\sigma_c^2 | 1, 0.1) \\
& \times \mathrm{IG}(\sigma_d^2 | 1, 0.1) \mathrm{IG}(\sigma_n^2 | 1, 0.1) \mathrm{IG}(\sigma_{fb}^2 | 1, 0.1) \\
& \times \mathrm{IG}(\sigma_{fp}^2 | 1, 0.1) \mathrm{IG}(\sigma_{gb}^2 | 1, 0.1) \mathrm{IG}(\sigma_{gp}^2 | 1, 0.1) \\
& \times \mathrm{IG}(\sigma_q^2 | 1, 0.1) \mathrm{IG}(\sigma_r^2 | 1, 0.1). \qquad (4.26)
\end{aligned}
$$

We chose our priors (as listed in equation (4.26)) to encompass the range of values we would expect for parameters (roughly based on data), but assured (with additional model fitting) that they were diffuse enough to have little effect on the means and credible intervals of the posterior densities of interest. Extremely diffuse priors run the risk of generating improper posteriors, which we wished to avoid. We centered priors of mean effects on zero, with the exception of slope parameters (G_b, G_p, R), which we gave slightly positive priors to reflect our belief that the relationship between the probability of detection (in clipstrips or percent cover quadrats) and abundance (biomass or percent cover) is also positive; and that the relationship between percent cover and biomass is also positive.

4.2.3 Model fitting

The joint posterior in equation (4.26) is analytically intractable, but posterior densities of the

parameters of interest can be estimated by simulating from conditional posteriors using MCMC. We implemented MCMC sampling using the statistical package WinBUGS version 1.4 (Bayesian inference Using Gibbs Sampling—http://www.mrc-bsu.ca.ac.uk/bugs). We initialized three chains from dispersed values, and found that all chains converged on the same parameter combinations. We assessed convergence visually as well as with the scale reduction factor of Gelman and Rubin, and found no evidence against convergence for any parameter. We discarded 5000 "burn-in" iterations, and thinned chains (by 1000) to reduce autocorrelation within chains to zero. After thinning and burn-in, posteriors were based on 500 samples.

4.3 Results

Because the 3094 total parameters across species, rings, and plots that we fit with our model precludes detailed discussion of all parameters, we briefly discuss model fitting of *A. gerardii*. *Andropogon gerardii* is a good example, because this species is abundant across our plots and also produces large numbers of inflorescences per plot (Figure 4.3(a,b,c)). Model fitting indicates that nitrogen strongly affects inflorescence production of *A. gerardii* (Table 4.1, Figure 4.4). Declining diversity decreases allocation to reproduction for this species, most strongly in the one-species plots (Table 4.1, Figure 4.4). These relationships are evident when examining the relationship between biomass (β_{ijk}) and inflorescences in ambient and elevated nitrogen plots (Figure 4.4(c,d)) and in plots at the four levels of diversity (Figure 4.4(e,f)). The relationship between expected biomass (β_{ijk}), percent cover (π_{ijk}), and inflorescences (ι_{ijk}) and observed data ($\bar{b}_{ijk}$, $\bar{p}_{ijk}$ and s_{ijk}) for *A. gerardii* suggests that our model adequately describes data for this species (Figure 4.5). Tight confidence intervals and low parameter correlations give confidence in parameter estimates of global change effects (results not shown). Only slope and intercept parameters (describing the relationship between observation probabilities and percent cover or biomass; and the relationship between percent cover and biomass—$f_{bi}, f_{pi}, g_{bi}, g_{pi}, q_i, r_i$) were strongly correlated for this as well as other species, as would be expected. Credible intervals for intercept parameters did overlap zero for a few species ($\sim$4), but credible intervals for slope parameters were always greater than zero.

Across all species, allocation to inflorescence production was reduced by elevated CO_2 (Tables 4.1 and 4.2, Figure 4.6). For most species, effects of elevated CO_2 were consistently negative, although 95% credible intervals of seven species overlap zero (χ_i; see Table 4.1, Figure 4.6). Across all species, the effect of elevated nitrogen on inflorescence production (N) was not different from zero (Table 4.2, Figure 4.6). The effects of elevated nitrogen on inflorescence production of individual species (ν_i), however, was positive for five species (*A. gerardii, B. gracilis, S. scoparium, S. rigida, L. capitata*) and negative for two species (*A. millefolium, P. pratensis*). Across all species, declining diversity (from 16 to 9, 4, or 1 species plots) did not have consistently positive or negative effects (Table 4.2, Figure 4.6). However, declining diversity positively affected allocation to inflorescence production (for at least one diversity level) for four species (*A. millefolium, B. gracilis, K. cristata, P. pratensis*), while negatively affecting three species (*A. gerardii, B. inermis, L. capitata*).

4.4 Discussion

The effects of CO_2, nitrogen, and diversity on allocation to inflorescence production of these twelve grassland species may strongly affect plant community dynamics, as theoretical models suggest that early life-history stages of plants play a pivotal role in structuring plant communities (Janzen 1970; Shmida and Ellner 1984; Warner and Chesson 1985; Tilman 1994; Hurtt and Pacala 1995; Chesson 2000). However, the manner in which shifts in allocation to reproduction will affect community structure is difficult to predict. For example, theoretical models demonstrate that low seed production can promote diversity by slowing competitive exclusion, if recruitment limitation constrains inter-specific competition (Shmida and Ellner 1984; Hurtt and Pacala 1995). It would be tempting to conclude that the generally negative effects of elevated CO_2 on allocation to inflorescence production (Table 4.2, Figure 4.6) could therefore allow more species to coexist in

Table 4.1 Posterior mean parameter estimates and 95% credible intervals (in parentheses) for parameters describing species-specific effects of global change on inflorescence production per unit biomass (as described by equations (4.3)–(4.5))

Functional group Species	Ambient inflorescence production (α_i)	Elevated CO_2 effects (χ_i)	Elevated nitrogen effects (ν_i)	Declining diversity effects (relative to 16-species plots)		
				9-species (δ_{9i})	4-species (δ_{4i})	1-species (δ_{1i})
C3 grasses						
Agropyron repens	−3.051 (−3.647, −2.384)	−0.302 (−0.742, 0.163)	−0.3644 (−0.8109, 0.06761)	0.01475 (−0.5593, 0.5489)	0.1937 (−0.4639, 0.8284)	0.1912 (−0.4386, 0.9043)
Bromus inermis	−2.735 (−3.207, −2.265)	−0.5851 (−1.045, −0.1296)	−0.3247 (−0.6238, 0.0074)	0.00871 (−0.3875, 0.3917)	−0.008894 (−0.3624, 0.3537)	−0.547 (−1.047, −0.04706)
Koeleria cristata	−2.602 (−3.170, −2.055)	−0.4433 (−0.8586, −0.0041)	−0.3408 (−0.7743, 0.04223)	−0.2538 (−0.8678, 0.2913)	−0.04722 (−0.6803, 0.4828)	1.205 (0.6496, 1.746)
Poa pratensis	−3.303 (−3.974, −2.702)	−0.5885 (−1.1620, −0.1130)	−0.5733 (−0.9038, −0.2290)	0.6858 (0.2633, 1.107)	0.09455 (−0.3931, 0.5822)	1.742 (1.266, 2.237)
C4 grasses						
Andropogon gerardii	−2.551 (−3.196, −1.949)	−0.3607 (−0.8197, 0.1292)	0.7462 (0.4296, 1.065)	−0.133 (−0.5353, 0.2462)	−0.2963 (−0.6943, 0.06335)	−0.9789 (−1.557, −0.4348)
Bouteloua gracilis	−1.891 (−2.598, −1.255)	−0.4782 (−0.9322, −0.0749)	0.8124 (0.4326, 1.223)	0.3356 (−0.2566, 0.8894)	0.8626 (0.2995, 1.372)	1.122 (0.401, 1.786)
Schizachyrium scoparium	−1.536 (−2.159,−0.993)	−0.4246 (−0.8732, 0.0034)	0.4385 (0.004913, 0.9289)	−0.4075 (−0.9246, 0.08268)	−0.177 (−0.7365, 0.3937)	−0.269 (−0.9325, 0.4038)
Sorghastrum nutans	−1.776 (−2.297, −1.210)	−0.2717 (−0.7364, 0.1578)	0.2067 (−0.1887, 0.5953)	−0.295 (−0.8634, 0.1927)	−0.4381 (−0.9388, 0.04781)	−0.4 (−0.9957, 0.207)
Forbs						
Achillea millefolium	−3.020 (−3.427, −2.619)	−0.4079 (−0.8049, −0.0477)	−0.4575 (−0.7113, −0.1858)	0.1925 (−0.1989, 0.5358)	0.4727 (0.1497, 0.7903)	0.5602 (0.05097, 0.9842)
Solidago rigida	−3.007 (−3.646, −2.416)	−0.2783 (−0.7247, 0.1994)	0.476 (0.1418, 0.8207)	0.1109 (−0.456, 0.7606)	−0.07574 (−0.6333, 0.4637)	0.02449 (−0.5904, 0.7057)
Legumes						
Lespedeza capitata	−2.419 (−2.871, −1.965)	−0.3432 (−0.7461, 0.06601)	0.629 (0.3207, 0.9883)	−0.258 (−0.6028, 0.09143)	−0.5275 (−0.9491, −0.0995)	−1.23 (−1.815, −0.6406)
Lupinus perennis	−1.803 (−2.192, −1.406)	−0.2503 (−0.6587, 0.1409)	−0.07445 (−0.3141, 0.1536)	0.04382 (−0.2084, 0.334)	−0.2905 (−0.5715, 0.02534)	−0.3467 (−0.8031, 0.09537)

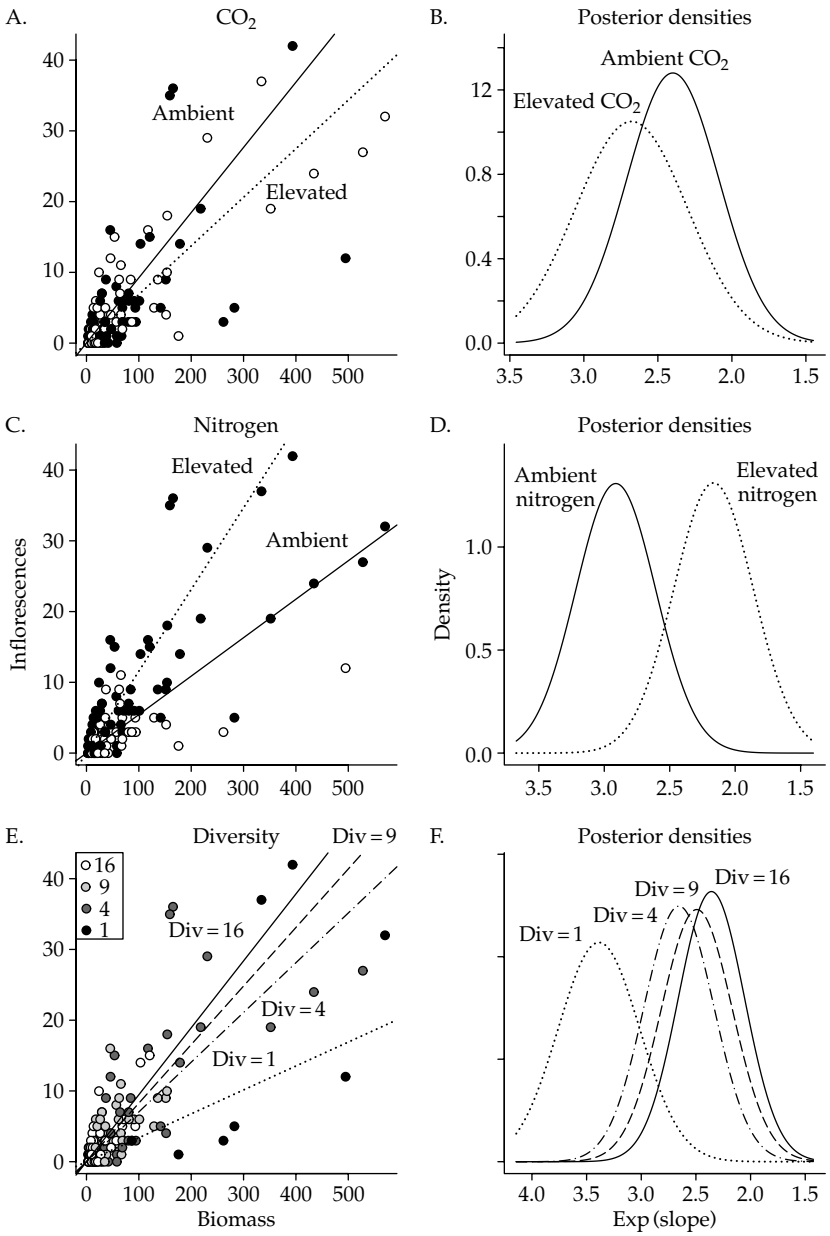

Figure 4.4. The effects of global change on per unit biomass inflorescence production of *A. gerardii*. In (a,c,e) we show the relationship between expected biomass and observed inflorescence production (β_{ijk} versus s_{ijk}) for ambient and elevated CO_2 rings (a), ambient and elevated nitrogen plots (c), and for plots at 16, 9, 4, and 1 levels of diversity (e). Open circles represent ambient CO_2 plots in (a), ambient nitrogen plots in (c), and 16 diversity plots in (e). Black circles represent elevated CO_2 in (a), elevated nitrogen plots in (c), and one diversity plots in (e). Dark gray circles in (e) represent four diversity plots, and light gray circles in (e) represent nine diversity plots. Superimposed lines show the expected relationships between biomass and inflorescence production under the various global change scenarios (based on posterior densities of treatment effects α_i, χ_i, ν_i, δ_{9i}, δ_{4i}, δ_{1i}). In (b,d,f) we show the posterior densities of per unit biomass inflorescence production (on the exponential scale) in ambient and elevated CO_2 rings (b), ambient and elevated nitrogen plots (d), and in plots at 16, 9, 4, and 1 levels of diversity (f).

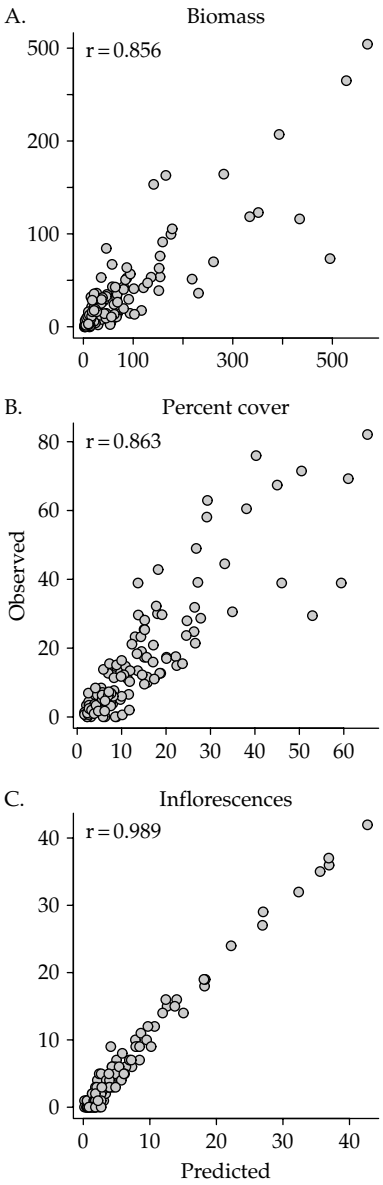

Figure 4.5. Comparisons of model predictions versus observations for *A. gerardii* biomass (a: β_{ijk} versus $\bar{b}_{ijk}$), percent cover (b: π_{ijk} versus $\bar{p}_{ijk}$), and inflorescences (c: ι_{ijk} versus s_{ijk}).

local habitats at Cedar Creek, because decreased inflorescence production should lead to increased recruitment limitation. However, seed production depends both on how much biomass species allocate to inflorescence production (examined in this chapter) as well as plant size and/or abundance, also affected by elevated CO_2. If the positive effect of elevated CO_2 on aboveground productivity (Reich et al. 2001) is greater than its' negative effects on allocation to inflorescence production on seed production, recruitment limitation may be decreased, not increased.

Of the three global change factors, elevated CO_2 had the most consistent effect, decreasing inflorescence allocation of all species (Table 4.2, Figure 4.6). The magnitude of effects does not appear to be linked to functional group status (Thurig et al. 2003). Although credible intervals overlap zero for many species, this may in part be due to the low replication of independent CO_2 treatments (Figure 4.1). Our results are consistent with those of a recent meta-analysis, which found that elevated CO_2 stimulates aboveground productivity (vegetative biomass) of plant species more strongly than their seed production, decreasing allocation to reproduction for a wide variety of plant species under elevated CO_2 conditions (Huxman et al. 1999; Jablonski et al. 2002; but see LaDeau and Clark 2001; Thurig et al. 2003). Why would allocation to reproduction decrease under elevated CO_2? Seed production of these perennial species may be more limited by nitrogen than carbon or water (seeds typically contain higher concentrations of nitrogen than vegetative biomass). Thus, when carbon and water become less limiting with elevated CO_2, increased photosynthates may be preferentially allocated to vegetative growth, not seed production.

Nitrogen had a strong positive effect on inflorescence production for some species (e.g. *A. gerardii*) and a strong negative effect on others (e.g. *A. millefolium*), leading to an overall effect (across all species) that was not different from zero (Table 4.2, Figure 4.6). The effects of added nitrogen on inflorescence production could be generalized for two functional groups: C4 grasses increased whereas C3 grasses decreased their per unit biomass inflorescence production under elevated nitrogen (Figure 4.6). This was opposite to the pattern we expected, suggesting that perennial species allocate less biomass to reproduction when resources become less limiting. Alternatively, life-history strategies correlated with these ecophysiological functional groups may better explain why species respond as they do. Three of the four C3 grasses

Table 4.2 Posterior mean parameter estimates and 95% credible intervals for overall treatment effects and overall (across species) variance parameters

Parameters (symbols)	Mean effect (95% credible interval)	Species-specific variance (95% credible interval)
Ambient inflorescence production (A, σ_a^2)	−2.461 (−2.864, −2.061)	0.3398 (0.162, 1.0302)
Elevated CO_2 effects (X, σ_c^2)	−0.394 (−0.6625, −0.133)	0.0528 (0.0214, 0.2144)
Nitrogen deposition effects (N, σ_n^2)	0.1018 (−0.2228, 0.472)	0.248 (0.1169, 0.7386)
Declining diversity effects: from 16 to 9 species (Δ_9, σ_d^2)	0.08727 (−0.3225, 0.5144)	0.3911 (0.2231, 0.7788)
Declining diversity effects: from 16 to 4 species (Δ_4, σ_d^2)	−0.02935 (−0.4673, 0.3923)	0.3911 (0.2231, 0.7788)
Declining diversity effects: from 16 to 1 species (Δ_1, σ_d^2)	−0.00014 (−0.3759, 0.3596)	0.3911 (0.2231, 0.7788)

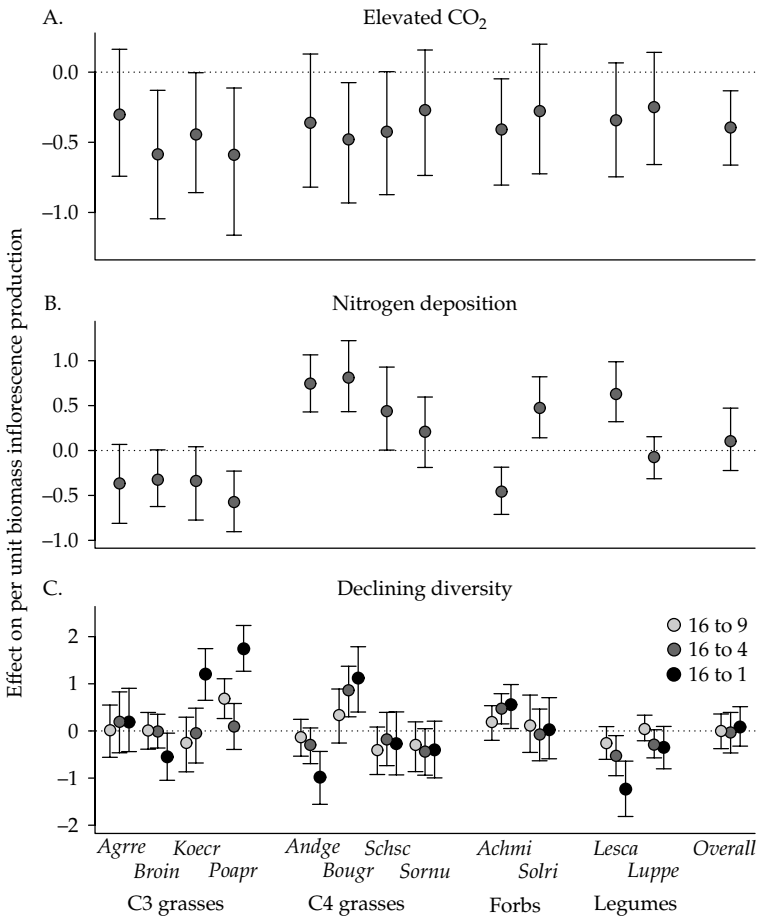

Figure 4.6. Posterior means and credible intervals of parameters describing the effects of elevated CO_2 (a), elevated nitrogen (b), and declining diversity effects (nine-, four-, and one-species plots; c) on the relationship between biomass and inflorescence production. The first 12 symbols in (a) and (b) represent species-specific estimates of treatment effects (χ_i, ν_i), and the 13th symbol represents average effects across all species (X, N). In (c), the first 36 symbols represent estimates of diversity treatment effects (δ_{9i}, δ_{4i}, δ_{1i}), and the 37th through 39th symbols represent average diversity effects across all species (Δ_9, Δ_4, Δ_1). The light gray symbols, dark gray symbols, and black symbols in (c) represent the nine-, four-, and one-species diversity treatments, respectively. Bars around symbols represent 95% credible intervals from Gibbs sampling. The horizontal dashed line marks zero (no effect). Species are organized by functional groups.

in this experiment can spread rapidly vegetatively through clonal growth (*A. repens, B. inermis, P. pratensis*). *Achillea millefolium*, another species whose reproductive allocation was depressed by elevated nitrogen is also clonal (Table 4.1, Figure 4.6). The four C4 grasses, however, rely on seeds to colonize empty space, as do *L. capitata* and *S. rigida*, species that also allocate more biomass to inflorescence production with elevated nitrogen. Perhaps plant species in these systems tend to allocate more biomass to structures that allow them to spread rapidly when nitrogen levels increase, but the identity of these structures (e.g. tillers versus seeds) differs between species (Gardner and Mangel 1999; Wand et al. 1999). Another interesting observation is that species that are active early in the growing season (*A. millefolium*, *A. repens*, *B. inermis*, *K. cristata*, *L. perennis*, *P. pratensis*) tended to be negatively affected by increased nitrogen, while late season species (*A. gerardii*, *B. gracilis*, *L. capitata*, *S. scoparium*, *S. rigida*, *S. nutans*) tended to be positively affected by increased nitrogen. Perhaps nitrogen is differentially limiting across the growing season, causing species-specific shifts in reproductive allocation to depend on when species are phenologically active.

As we had expected, declining diversity increased (*A. millefolium, B. gracilis, K. cristata, P. pratensis*) as well as decreased (*A. gerardii, B. inermis, L. capitata*) allocation to reproduction of grassland species (Table 4.1, Figure 4.6). These shifts in reproductive allocation with diversity are likely caused by the indirect effects of diversity on biotic and abiotic factors (e.g. pathogens, mutualists, soil resources). Species that increased allocation to reproduction with declining diversity are potentially responding to higher levels of limiting resources (e.g. water, nitrogen—Tilman et al. 1996), lower inter-specific competition, or increased densities of mutualists at low diversity (Burrows and Pfleger 2002). Conversely, species whose allocation to reproduction declines with diversity may be responding to greater intra-specific competition or higher pathogen loads (Mitchell et al. 2002). Because there are no obvious traits that unite those species increasing or decreasing allocation to reproduction with declining diversity, it is unlikely that all species are responding to the same underlying factors that vary with diversity. Additional observations or experiments testing specific mechanisms are needed to fully understand the indirect effects of diversity on allocation to seed production.

Despite the fact that the BioCON experiment was designed with classical frequentist statistical approaches in mind, the Bayesian hierarchial model presented here offers several advantages over more traditional analytical approaches. First, we were able to accommodate nonnormal data (e.g. our counts of inflorescences). Although generalized linear models can similarly accommodate nonnormally distributed data, specifying a myriad of different distributions for parameters and data alike (as can be done with Bayesian approaches, where both data and parameters are considered random variables) is not easily achieved with classical approaches. Second, we were able to estimate treatment effects while accounting for multiple hierarchical levels of stochasticity (i.e. plot, ring, and species random effects). We were also able to incorporate detection error that affected our covariates (biomass and percent cover) into our statistical models. Finally, we were able to incorporate two independently measured but correlated metrics of species abundance (percent cover and biomass), which, to our knowledge, is impossible using frequentist approaches. These aspects (nonnormal data, multiple hierarchical sources of variabilility, and multiple data sources) are not uncommon in ecological data sets. Thus, we believe that the analysis of data sets from many manipulative experiments will benefit from a Bayesian hierarchical approach (Ellison 2004; Clark 2005).

Predicting how changes in reproductive allocation will affect community structure requires increased efforts in empirical and statistical ecology. We lack data documenting recruitment responses of plants to global change, as most studies of the effects of global change factors such as CO_2, N, and diversity on plant communities measure vegetative biomass, not life-history transitions such as reproduction. This can be remedied by broadening the types of data being collected from experimental manipulations of global change factors in plant communities. There has been a strong focus on using ecophysiological traits such as photosynthetic pathway (C3 versus C4) and N-fixing capability (Legumes) to generalize how species will respond to global change; as our data illustrates, these functional groups are

not always useful for generalizing how all metrics of interest will respond to global change factors (Lavorel and Garnier 2002, Figure 4.6). An alternative approach would be to categorize species into functional groups using traits that depend on the global change factor and response variable of interest (e.g. photosynthetic pathway when determining the effects of elevated CO_2 on aboveground productivity—Poorter and Navas 2003; mating system and dispersal mode when determining the effects of fragmentation on seed set—Oostermeijer et al. 2003). Finally, we believe that hierarchical Bayesian models represent a promising tool for ecologists attempting to understand how global change will affect plant recruitment, and ultimately, community structure.

Acknowledgments

We thank Susan Barrott, Louise Bier, Dan Bahauddin, Teia Finch, Jenny Goth, Stan Harpole, Bill O'Gorman, Stefan Schnitzer, Jared Trost and Cedar Creek BioCON interns for assistance in the field. This work was supported by a US DOE Grant (DOE/DE-FG02-96ER62291) to Peter Reich.

PART III

Spatial modeling

Space enters environmental models as part of the "process," the "error," or both. In principle, the process of interest would take up spatial relationships, in the sense that movement may be an explicit element of the process model. The spatial autocorrelation not explained by the process model appears as 'leftover' variance, critical for proper inference, but in and of itself, not necessarily illuminating. In Chapter 5, Gelfand et al. provides an example where hierarchical Bayes allows for a sophisticated treatment of spatial autocorrelation. Inference on the factors that control species occurrence is not fully explained by covariates. Failure to allow for this error structure would result in the interpretation that covariates are more important than they are.

Ogle et al. allow for the spatial relationships that can affect inference on tree damage from hurricane winds. Here, hierarchical models allow for demographic rates at one stage, which depend on location. Spatial relationships are not modeled as part of the process, but rather allow for inference on the dynamics of forest change.